
Intelligent identification method for drilling conditions based on artificial neural networks

Received: 17 November 2025

Accepted: 26 December 2025

Published online: 16 January 2026

Cite this article as: Li W., Yang Y., Fan D. *et al.* Intelligent identification method for drilling conditions based on artificial neural networks. *Sci Rep* (2025). <https://doi.org/10.1038/s41598-025-34242-6>

Wei Li, Yuan Yang, Donglin Fan & Yuxing Zhou

We are providing an unedited version of this manuscript to give early access to its findings. Before final publication, the manuscript will undergo further editing. Please note there may be errors present which affect the content, and all legal disclaimers apply.

If this paper is publishing under a Transparent Peer Review model then Peer Review reports will publish with the final article.

Intelligent identification method for drilling conditions based on Artificial Neural Networks

Wei Li¹, Yuan Yang², Donglin Fan³, Yuxing Zhou^{4*}

¹ CHN Energy Shendong Coal Group Corporation Ltd., Production Management Department, Ordos, Inner Mongolia, 017209, China

² CHN Energy Shendong Coal Group Geodesy Company, Ordos, Inner Mongolia, 017209, China

³ CHN Energy Shendong Coal Group Technology Research Institute, Ordos, Inner Mongolia, 017209, China

⁴Jinneng Holding Equipment Manufacturing Group Cortech Shanxi Energy Technology Co., LTD, Jincheng, 102600, China

Correspondence to: Yuxing Zhou (3079324563@qq.com)

Abstract: Drilling efficiency analysis typically relies on manual post-event analysis, which is subjective and arbitrary, failing to accurately reflect real-time field conditions in a timely manner. To enable real-time, accurate, and automatic identification of drilling conditions and improve drilling efficiency, the authors developed an intelligent identification model based on artificial neural networks. Using Pearson correlation coefficient for correlation analysis, eight drilling parameters from comprehensive logging data were selected as input for network training: well depth, bit position, hook height, hook load, weight on bit, rotary speed, torque, flow rate, and standpipe pressure. By comparing the performance of Long Short-Term Memory (LSTM) neural networks, BP, and CNN in real-time intelligent identification of drilling conditions in deep formations, it was found that LSTM outperformed the others. The LSTM model achieved a recognition accuracy of 97%, demonstrating its efficiency and reliability while providing important theoretical and technical support for effective drilling condition identification.

Keywords: Neural Networks; Machine Learning; Drilling Conditions; Intelligent Identification; Prediction

0 Introduction

Drilling is a multifaceted and high-risk process due to the complexity and interdependence of its numerous stages and parameters. During operations, various drilling conditions such as pipe connection and tripping are encountered, each imposing specific requirements on drilling equipment and drilling fluid parameters. Failure to accurately identify the current drilling conditions may lead to improper operations, thereby causing drilling accidents. Therefore, accurate identification of drilling conditions is a critical measure to ensure the safety of drilling operations and improve their efficiency [1-3]. Drilling condition identification technology is one of the key technologies in drilling automation and intelligence. Real-time monitoring and

identification of different operational conditions during drilling help accurately analyze drilling efficiency, enhance drilling performance, and ensure operational safety, providing decision support and operational guidance for on-site construction [4-6]. Traditional drilling condition identification methods rely on real-time mud logging data trends and expert threshold rules for recognition. However, the threshold rule method has certain limitations in practical applications, manifesting as complex judgment logic, ambiguous threshold boundaries, and low identification accuracy for conditions with indistinct features. Traditional drilling condition identification methods rely on real-time mud logging data trends and expert threshold rules for recognition. However, the threshold rule method has certain limitations in practical applications, manifesting as complex judgment logic, ambiguous threshold boundaries, and low identification accuracy for conditions with indistinct features.

Some scholars have conducted relevant research on identification of drilling condition. For the field of neural networks, Yang used principal component analysis to reduce the dimensionality of feature parameters and then employed an artificial neural network to detect gas kicks [2]. Osarogiagbon utilized a long short-term memory recurrent neural network to learn the temporal relationships in time-series data composed of D-exponent data and riser pressure data, achieving early kick detection [7]. Muojek combined **artificial neural networks (ANN)**, binary classifiers, and downhole drilling flow parameter detection to establish a data-driven kick detection model [8]. Sun proposed a real-time intelligent drilling condition identification method based on support vector machines, addressing multi-classification problems by combining multiple SVMs [9]. Hou performed data cleaning and sample labeling, adopting an artificial neural network-based technique to identify nine common drilling conditions, including pipe connection, tripping out, tripping in, reaming up, reaming down, circulation, rotary drilling, slide drilling, and others [10]. For the field of machine learning, Li proposed an intelligent early kick identification method based on **Support Vector Machines (SVM)** and D-S evidence theory, introducing a posterior probability output model on the foundation of traditional SVM [1]. Liu Gang built upon conventional drilling anomaly warning methods and **established adaptive models of SVMs based on multi-source information and kernel-function**, effectively improving the accuracy of drilling incident and complexity warnings [11]. Liu proposed an intelligent drilling condition identification method based on decision trees, which to some extent meets the demands of oilfield digitalization and intelligence [12]. Mao proposed a drilling condition identification method based on the gradient boosting decision tree algorithm, using a moving window approach to select the optimal window for enhancing data stability, achieving significant results [13].

Although some progress has been made in utilizing machine learning and artificial neural networks to establish identification models for drilling conditions, the following limitations still exist [14]. The theory of BP neural networks makes it difficult to determine how to adjust

weights to reduce errors, and it requires relatively high data accuracy. When drilling conditions (such as kick, lost circulation, drill string washout, nozzle blockage, and other complex conditions) are not well linearly separable, the resulting model performs poorly. **SVM** do not suffer from local minima issues, but for large-scale training data, the transposition of high-dimensional matrices consumes significant machine memory and computational time [15]. Multi-layer SVM is a potential method for solving multi-classification problems, but it is difficult to implement for large-scale training samples and is sensitive to missing data [16]. **Random Forests (RF)** do not yield good classification results with small datasets or low-dimensional data, and when the number of decision trees is high, the model runs slowly, making it unsuitable for drilling condition identification projects with high real-time requirements [17]. The author conducted a comparative analysis of the adaptability of drilling condition identification algorithm models using field-collected drilling data. By evaluating the advantages and disadvantages of BP, CNN, and LSTM models, the effectiveness and adaptability of the proposed approach were validated.

1 Optimal selection of prediction methods of drilling conditions

1.1 Manual experience-based methods for drilling conditions

Comprehensive mud logging data serves as an effective approach for production control centers to achieve dynamic monitoring of field operations. By summarizing data trends and threshold ranges of drilling conditions based on drilling experience, and utilizing continuously measured drilling engineering parameters, real-time monitoring of drilling site conditions can be realized. Currently, manual experience-based methods can identify five drilling conditions: set slips, drilling, tripping out, tripping in, and maintaining the original condition. In this workflow discrimination chart, only four key parameters, inlet flow rate, hook height, hook load, and bit position, along with two threshold parameters, standard well depth and set slip threshold, are required for condition judgment. The flowchart for manual experience-based drilling condition judgment is shown in Fig. 1 below.

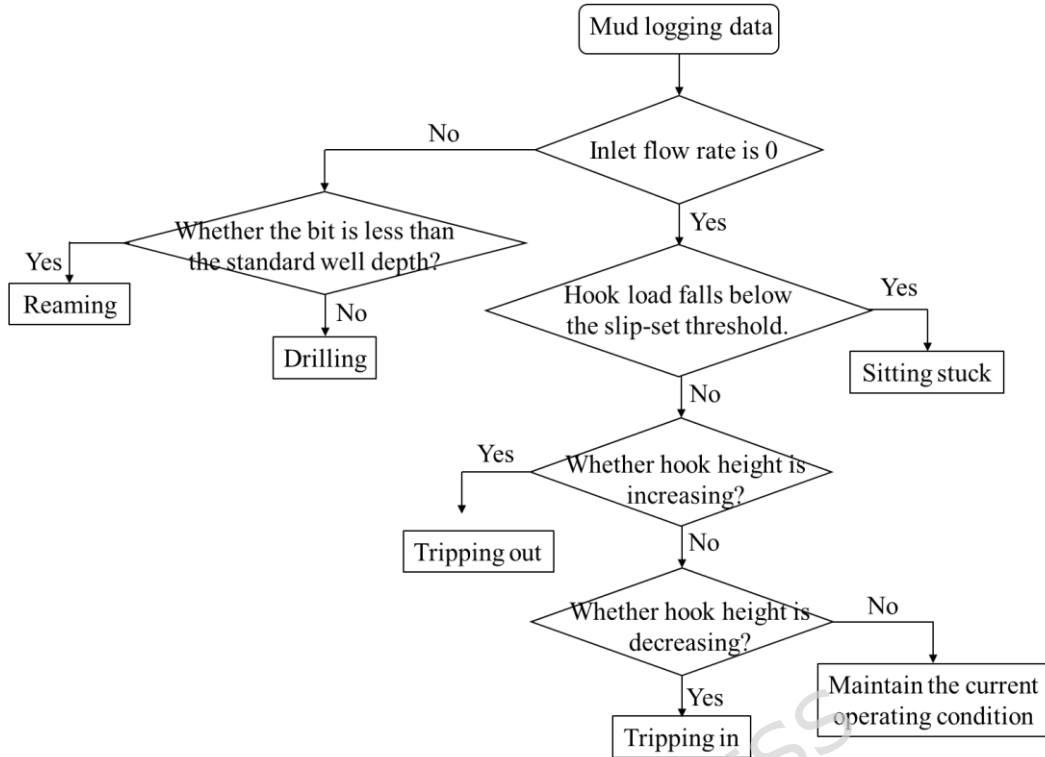


Fig. 1 Flowchart of experience-based identification of drilling conditions

1.2 BP Neural Network

The BP neural network is a multi-layer feedforward network trained according to error backpropagation algorithm, and is one of the most widely applied neural network models (Fig. 2). Its fundamental principle involves continuously adjusting the weights and thresholds of the network through forward propagation of input signals and backward propagation of errors, thereby minimizing the output error of the network.

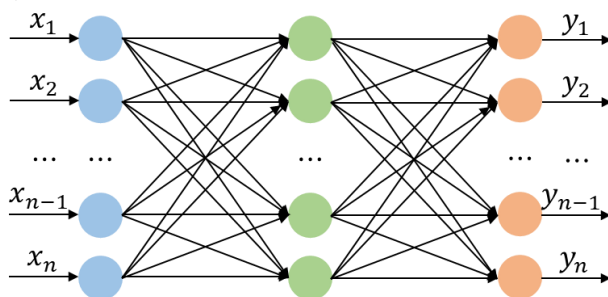


Fig. 2 Structure of the BP Neural Network

ANN are numerical computation-based knowledge processing systems, inspired by the structure of biological neural networks in the human brain. As a machine learning model, they consist of numerous simple processing units interconnected to form a complex network. The primary task for achieving intelligent identification of drilling conditions is to select the most suitable neural network algorithm based on the characteristics of the sample dataset. Subsequently, evaluation metrics such as accuracy, precision, recall, and F1 score are used to assess the classification performance of the machine learning model. The overall workflow for

predicting drilling conditions using artificial neural networks is illustrated in Fig. 3 below.

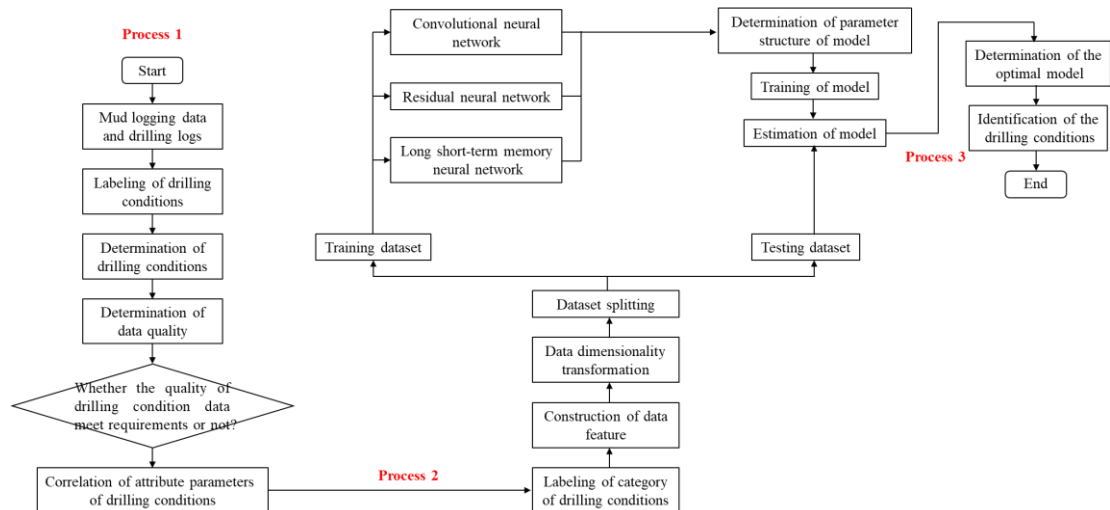


Fig. 3 The workflow based on neural network for the identification of drilling conditions

Drilling condition identification falls under the category of “classification” in supervised learning. Supervised learning is the process of adjusting the parameters of a neural network classifier using labeled samples to achieve the desired performance. The primary goal of a supervised learning model is to discover the relationship between input variables and output variables from data. By establishing this relationship, new data can be fed into the trained model to predict the values of the output variables. In this context, labeled samples (e.g., eight types of drilling conditions) are used to train the model parameters, which are then employed for training the neural network model.

In the context of drilling condition identification, the BP neural network can learn complex nonlinear relationships between drilling parameters (such as hook load, pump pressure, torque, etc.) and downhole conditions. During training, sample data is used to iteratively correct the network’s connection weights. Once training is complete, the model can effectively identify downhole conditions like kicks, lost circulation, and stick-slip. However, the BP neural network also has certain limitations. **Actually**, it is prone to falling into local minima, relies heavily on a large amount of high-quality training data, has a network structure that is difficult to determine theoretically, and exhibits poor generalization ability when dealing with small sample sets. In practical drilling applications, these factors must be carefully considered in the design and optimization of the network.

1.3 Long short-term memory network (LSTM)

Based on the long-time-series characteristics required for intelligent drilling condition identification, this study conducts structural analysis and comparative principle evaluation of three common neural network algorithms, thereby establishing an algorithmic foundation for intelligent drilling condition discrimination.

RNN is one of the most frequently used deep learning models for processing temporal sequence problems. Its architecture incorporates the hidden layer nodes from the previous time step $t-1$

as input for the current time step t , granting its exceptional performance in handling sequential data. However, the RNN's chain structure, which uses identical parameters across all time steps, makes it susceptible to the vanishing gradient problem during training. Gradients can diminish to zero, leading to what is known as the “long-term dependency” issue. This means that as the time interval increases, the RNN loses its ability to learn information from distant time steps. Consequently, the standard RNN is not suitable for intelligent drilling condition identification, which inherently involves long-time-series characteristics.

In 1997, Hochreiter and Schmidhuber proposed the LSTM-RNN model and demonstrated that the LSTM possesses the capability to remember both long- and short-term information, effectively resolving the long-term dependency problem of traditional RNNs. Recently, LSTM have undergone rapid development and have been successfully applied in the field of petroleum engineering. For instance, in 2019, Lee successfully predicted shale gas production using the LSTM.

Through detailed analysis of the structures of BP, RNN, and LSTM, and considering the long-time-series nature of comprehensive mud logging data, the LSTM, which excels at learning temporal sequence information and handling long-range dependencies, has been selected as the optimal algorithm for intelligent drilling condition identification.

The LSTM is a significant improvement upon RNN, replacing the standard neurons in the traditional RNN hidden layer with LSTM memory cells. When unfolded, the LSTM is equivalent to a feedforward neural network, where the input of each layer serves as the input for the next, and parameters are shared across all layers. The basic structure of the LSTM network is shown in Fig. 4. Its fundamental unit contains three gates, namely, the input gate, the forget gate, and the output gate. These three gates establish a self-loop mechanism within the internal state of the LSTM. Specifically: 1) The input gate determines how the current time step's input and the previous time step's internal state are updated; 2) The forget gate controls how much of the previous internal state is retained or forgotten for the current time step; 3) The output gate governs the extent to which the internal state influences the final output of the system. This architecture allows the LSTM model to capture parameter information at the current moment while retaining the changing trends of historical parameter information. The key reason LSTM can solve the long-term dependency problem of RNNs lies in its introduction of the forget gate f_t , input gate i_t , and output gate o_t to regulate the flow and loss of features.

The unfolded chain structure of the LSTM is depicted in Fig. 4.

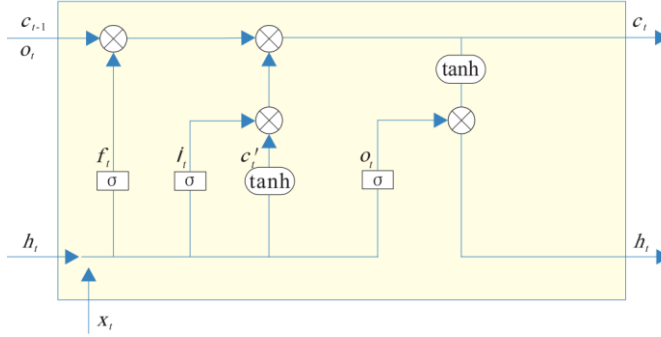


Fig. 4 Operational Principle of the LSTM Network’s Recurrent Unit at Time Step t

In Fig. 4, the long horizontal line running from left to right at the top allows learned knowledge to pass directly along it without easy alteration, thereby enabling the LSTM network to possess “long-term” memory and solving the “long-term dependency” problem of RNNs. The combined use of “short-term memory” and “long-term memory” allows LSTM to learn both “short-term” and “long-term” patterns over long sequences. When the long-term cell state passes through the neural network, the forget gate f_t “forgets (deletes)” part of the memory information, the input gate i_t “inputs (adds)” part of the memory information, and finally, after processing by the output gate, the result is output. Fig. 4 shows the structure of the recurrent unit of the LSTM network at time step t . As shown in Fig. 1, the output of the hidden layer at time $t-1$ and the input at time t are first copied into four parts each, and different weights are randomly initialized. Then, h_{t-1} and x_t vectors are concatenated. Finally, nonlinear transformation is performed through the activation functions (sigmoid or tanh) to obtain the activation vectors for the forget gate, input gate, output gate, and the transformed cell state vector. The calculation formulas are as follows:

$$f_t = \sigma(W_f \cdot [h_{t-1}, x_t] + b_f) \quad (1)$$

$$i_t = \sigma(W_i \cdot [h_{t-1}, x_t] + b_i) \quad (2)$$

$$o_t = \sigma(W_o \cdot [h_{t-1}, x_t] + b_o) \quad (3)$$

$$c_t' = \tanh(W_c \cdot [h_{t-1}, x_t] + b_c) \quad (4)$$

Where: f_t , i_t , and o_t are the activation vectors of the forget gate, input gate, and output gate at time step t , respectively; c_t' is denotes the cell state candidate vector at time step t , obtained after transformation through the tanh layer. W is the weight matrix associated with different

stages. \mathbf{b} is the bias vector associated with different stages. \mathbf{x}_t is the input at time step t . \mathbf{h}_{t-1} is the output of the hidden layer at the previous time step $t-1$. σ is the sigmoid activation function.

These components work together within the LSTM architecture to regulate information flow, enabling the network to effectively capture and retain long-term dependencies in sequential data. The forget gate f_t and input gate i_t is used to discard part of the useless stored information and retain part of the useful information at time t , thereby updating the internal memory cell c_t .

The calculation formula is as follows:

$$\mathbf{c}_t = f_t \cdot \mathbf{c}_{t-1} + i_t \cdot \mathbf{c}_t' \quad (5)$$

Where: \mathbf{c}_t is the updated memory cell at time t ; \mathbf{c}_{t-1} is the preserved memory cell from the previous time step $t-1$. The output gate o_t selects useful information from \mathbf{c}_t and transmits it to the hidden state \mathbf{h}_t . The calculation formula is as follows:

$$\mathbf{h}_t = o_t \cdot \tanh(\mathbf{c}_t) \quad (6)$$

Where: \mathbf{h}_t is output of the hidden layer at time t .

2 Performance evaluation metrics for machine learning models

Generally, the generalization error is used to evaluate the performance of a machine learning model. A smaller generalization error indicates better model performance. The test set is employed to assess the model's classification and discrimination capabilities, and the test error from the test set is used as an approximation of the generalization error. This paper adopts four evaluation metrics: Accuracy, Precision, Recall, and F1-score. Based on the actual categories and the model's predicted categories, the classification results are organized. The confusion matrix for binary classification is shown in Table 1, and the confusion matrix for multi-class classification is shown in Fig. 5. Here, TP represents true positives, FP represents false positives, TN represents true negatives, and FN represents false negatives.

Table 1 Confusion matrix of binary classification results

Actual values	Predicted values	
	Positive	Negative
True	TP	FN
False	FP	TN

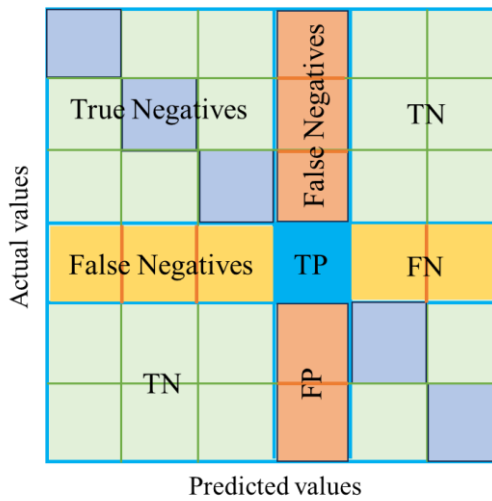


Fig. 5 Confusion matrix for multi-class classification problem

Different metrics directly reflect the performance of classification. “Accuracy” is the most common evaluation criterion, which is the number of correctly classified samples divided by the total number of samples. For balanced classification problems, a higher accuracy generally indicates a better classifier. “Precision” and “Recall” are a pair of contradictory metrics. “Precision” reflects how many predictions for a certain class are correct and how many are incorrect. “Recall” shows how many of the predictions for a certain class are correct. The “F1-score” is the harmonic mean of precision and recall.

3 Dataset description and organization

3.1 Types of mud logging data

The data was sourced from actual drilling operations in the Western Mining Area. A comprehensive mud logging unit collected over 100 drilling parameters, including time, well depth, and bit position, resulting in a total of 2 million recorded data entries. The extensive parameters in the mud logging data can be categorized into three types: drilling parameters, drilling fluid parameters, and gas logging parameters. The specific classifications and details are presented in Table 2.

Table 2 The types of parameters of composite mud logging

Composite data	Content of data
Drilling parameters	Well depth, Bit position, Hook height, Hook load, Weight on bit, Rotary speed, Torque, Flow rate, Standpipe pressure
Drilling fluid parameters	Inflow/outflow drilling fluid density, Inflow/outflow drilling fluid temperature
Gas logging parameters	Total hydrocarbons, Methane, Hydrogen sulfide

3.2 Data normalization

1) Abnormal data processing

In mud logging data, sensor interruptions or distortions may result in abnormal data points with

a fixed value of “-999”. To prevent these anomalous values from adversely affecting model accuracy, this study employs the method of directly removing entire rows containing such abnormal values. Given that the drilling time-series data in this research has a sampling interval of 4-5 seconds, the dataset is sufficiently large, and the frequency of abnormal values is relatively low. Removing these data points does not significantly impact the continuity or overall integrity of the dataset.

Furthermore, as sensor data from the near-wellbore region tend to exhibit substantial distortions, this study excludes logging data from the first 1000 meters to further enhance data quality and reduce interference in model training. Only data beyond 1000 meters is used for model training and analysis. This processing strategy effectively improves data reliability and model robustness.

2) Data normalization processing

Data normalization is a commonly used data preprocessing operation aimed at handling data of different scales and dimensions, scaling them to the same data range and scope to reduce the impact of scale, features, and distribution differences on the model. Common data normalization methods include Z-Score and min-max. Considering that drilling is a sequential process that varies with depth, parameters such as well depth and drilling pressure do not follow a normal distribution. To eliminate dimensions and reduce the impact of different magnitudes of parameters on model performance, this study adopts the min-max normalization method to linearly transform the original logging data, constraining the data to the range [0, 1], namely:

$$x^* = \frac{x - x_{\min}}{x_{\max} - x_{\min}} \quad (7)$$

Where: x^* is the normalized value; x_{\max} is the maximum value in the training data; x_{\min} is the minimum value in the training data.

3.3 Correlation analysis

In the actual drilling process, various logging parameters are not isolated from each other; there exists a certain causal relationship among them. Correlation analysis involves calculating the correlation coefficient between datasets to determine the changing characteristics between two parameters. Generally, it can be categorized into two types of relationships: positive correlation and negative correlation. A positive correlation indicates that as one parameter increases, the other also increases, and as one decrease, the other decreases. Conversely, a negative correlation implies the opposite. Through correlation analysis of data, parameter relationships can be quickly identified, and key parameters can be extracted. Commonly used correlation

coefficients include the Pearson correlation coefficient and the Spearman correlation coefficient.

(1) Pearson correlation coefficient

The Pearson correlation coefficient is generally used to analyze the relationship between two continuous variables and is a linear correlation coefficient. The formula is:

$$r_p = \frac{\sum_{i=1}^n (x_i - \bar{x})(y_i - \bar{y})}{\sqrt{\sum_{i=1}^n (x_i - \bar{x})^2 \sum_{i=1}^n (y_i - \bar{y})^2}} \quad (8)$$

Where: r_p is the Pearson correlation coefficient value between two drilling parameters. A value greater than 0 indicates a positive correlation, while a value less than 0 indicates a negative correlation; n is the number of drilling parameters; x_i, y_i are the recorded values of the two drilling parameters; \bar{x}, \bar{y} are mean value of drilling parameters.

(2) Spearman correlation coefficient

The Pearson correlation coefficient requires that the values of continuous variables follow a normal distribution. For variables that do not follow a normal distribution, or for measuring associations between categorical or ordinal variables, Spearman's rank correlation coefficient, also known as the rank correlation coefficient, can be used. The formula is:

$$r_s = 1 - \frac{6 \sum_{i=1}^n (R_i - Q_i)^2}{n(n^2 - 1)} \quad (9)$$

Where: r_s is the Spearman's rank correlation coefficient between two drilling parameters. A value greater than 0 indicates a positive correlation, while a value less than 0 indicates a negative correlation. n is the number of drilling parameters. The paired values of the two variables are ranked in ascending (or descending) order, respectively. R_i is the rank of x_i ; Q_i is the rank of y_i ; $(R_i - Q_i)$ is the difference in ranks between x_i and y_i .

To ensure that the selected working condition parameters are independent yet exhibit a certain degree of correlation, the Pearson correlation coefficient was used for analysis. As shown in Fig. 3, which presents the Pearson correlation coefficient plot of the working condition parameters, the horizontal and vertical axes represent each drilling parameter variable listed in the table. The value at the intersection of the horizontal and vertical axes indicates the correlation between two drilling parameter variables. The closer the absolute value is to 1, the stronger the correlation between the two parameters. In the plot, darker shades indicate a higher degree of correlation, while lighter shades indicate greater independence between the two

parameters. Negative values indicate a negative correlation between the two parameters. Larger absolute values signify a stronger correlation, while smaller absolute values indicate weaker correlation and greater independence between the two parameters.

As can be seen from Fig. 6, eight drilling parameters in the comprehensive logging data, such as well depth, bit position, hook height, hook load, weight on bit, rotary speed, torque, flow rate, and standpipe pressure, exhibit strong correlations. Therefore, these eight logging parameters were selected as feature parameters for model training to accurately identify eight drilling conditions, including rotary drilling, sliding drilling, downward washing, reaming, upward washing, back reaming, tripping out, and tripping in.

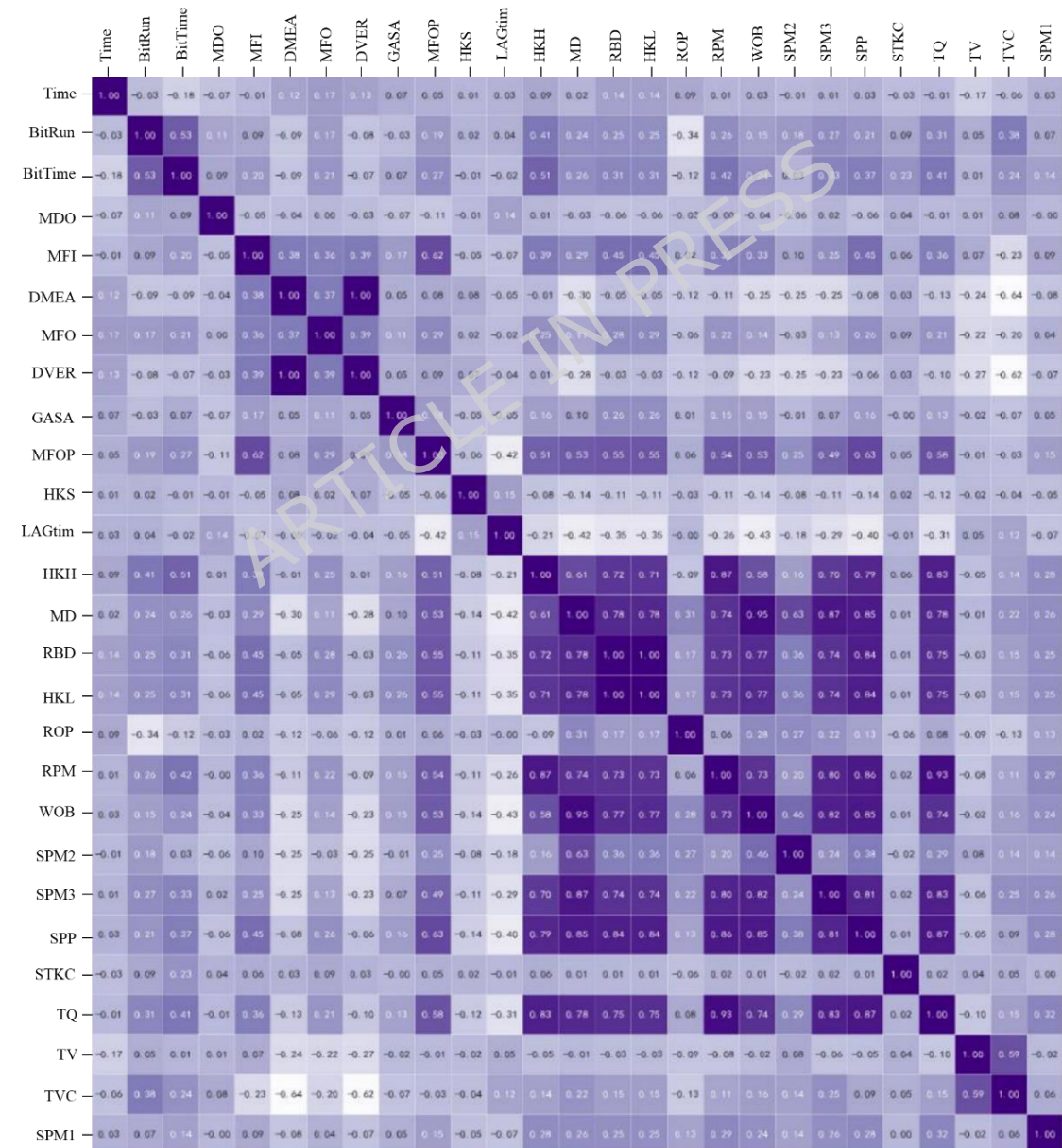


Fig. 6 Drilling parameter correlation heatmap

3.4 Sample data labeling

A sample set for working condition identification, as shown in Table 3, was established based on the collected drilling dataset. The drilling condition at each time point serves as the output for network training. However, the drilling condition status cannot be directly obtained from the drilling dataset. Therefore, before model training, the drilling conditions must be manually labeled with reference to drilling logs. The data distribution and labels for the eight drilling conditions used in the classification task are shown in Table 3. It can be observed that the data distribution for three drilling conditions, sliding drilling, stationary, and downward washing, accounts for less than 5% of the total, indicating an imbalanced classification problem. Consequently, recall rates will need to be analyzed in subsequent steps.

Table 3 Statistical analysis of sample dataset

Drilling parameters	Minimum	Maximum	Mean	Standard deviation
Bit depth/m	0	5286.22	2025.32	450.35
Measured depth/m	552.00	5286.45	2621.57	398.38
Hook height/m	1.53	39.58	15.76	4.78
Weight on bit/kN	0	279.85	90.55	26.89
Hook load/kN	0	4956.79	998.53	202.75
RPM/(r·min ⁻¹)	0	175.00	70.36	15.97
Torque/(kN·m)	0	55.67	16.45	4.19
Standpipe Pressure/MPa	0	50.88	13.71	3.16

The comprehensive logging dataset from deep formations used in this section contains a total of 20,000,000 rows of sample data. Among these, 75% is allocated as the training set and 25% as the test set. Algorithms are then employed for learning and validation to achieve classification and prediction of drilling conditions. The manual labeling rules for the eight typical drilling conditions are detailed in Table 4, while the remaining logging data from deep formations corresponding to other drilling conditions are labeled as “Other”.

Table 4 Labeling rules for the eight typical drilling conditions

Drilling conditions	Data volume	Distribution of data volume (%)	Label	One-hot Encoding
Rotary drilling	9 125 378	40.09	0	100 000 00
Sliding drilling	492 549	2.16	1	010 000 00
Downward washing	890 724	3.91	2	001 000 00
Reaming	2 950 845	12.97	3	000 100 00
Upward circulation	885 973	3.89	4	000 010 00
Reverse reaming	2 659 467	11.69	5	000 001 00
Tripping out	3 225 795	14.18	6	000 000 10
Tripping in	2 525 879	11.00	7	000 000 01
Total	22 756 610	100		

4. Network structure and parameter settings

4.1 BP neural network structure and hyperparameter settings

Table 5 Parameter settings of BP

Parameters	Values
Normalization	StandardScaler
Number of input layers	32

Number of neurons of hidden layers	128
Number of neurons of output layers	2
Initial learning rate	0.001
Activation function	Relu
Optimizer	Adam
Iterations	400

Table 5 presents the network architecture and parameter settings summarized through multiple experiments. The value range of standard well depth in drilling data is not fixed, so standard normalization was selected to process the input data. The original drilling data had 33 features. After removing the irrelevant time field, 32 features remained as network inputs. The hidden layer was **configured** with 128 neurons to achieve better network convergence. Since the network output is a binary classification, the output layer was set with 2 neurons. The learning rate should not be set too high, as an excessively large value might cause the model to skip the global optimum and fail to converge. A learning rate of 0.001 was chosen to ensure final model convergence. The ReLU activation function was used due to its simple derivative calculation, reduced computational time, and absence of gradient vanishing issues. The Adam optimizer was selected for its relatively shorter computational time, and the number of iterations was set to 400.

4.2 Structure and hyperparameter settings of LSTM

Based on multiple experimental results, **the architecture and hyperparameter settings of LSTM** are summarized in Table 6. The normalization method selected was StandardScaler. The sequence length was set to 6, as this value was determined to be optimal based on label continuity. The feature dimension is 32, with 128 neurons in each LSTM cell. The ReLU activation function was chosen, and the hidden layer **was configured with 128 neurons**. The output layer consists of 2 neurons. The initial learning rate was set to 0.01, the Adam optimizer was selected, and the number of iterations was set to 100.

Table 6 LSTM Neural Network Parameter Settings

Parameters	Values
Normalization	StandardScaler
Length of sequence	6
Feature dimension	32
The number of neurons in the Cell	128
Activation function	Relu
Number of neurons of hidden layers	128
Number of neurons of output layers	2
Initial learning rate	0.01
Optimizer	Adam
Iterations	100

5 Comparison

5.1 BP neural network experimental results

(1) Loss curve analysis

The loss variations during the training process for each drilling condition are shown in Fig. 7. The loss value for each condition decreased rapidly at the beginning of training, indicating that the model effectively learned the patterns for condition identification. Around 200 iterations, the loss curve stabilized, demonstrating that setting the total number of iterations to 400 was reasonable. The loss values eventually converged to approximately 0.3, reflecting successful training outcomes.

(2) Analysis of accuracy, precision, recall, and F1-Score of the model

The statistical results for accuracy, precision, recall, and F1-Score of these seven BP neural network models are presented in Table 7. The average F1-Score of the BP neural network models reached 0.9694, indicating that the trained models possess strong recognition capabilities. This step also ensures the objectivity and accuracy of the subsequent analysis of high-weight fields for drilling conditions.

Table 7 Evaluation of BP neural network models

Drilling conditions	Accuracy	Precision	Recall	F1 score
Rotary drilling	0.9261	0.9236	0.9433	0.9518
Slide drilling	0.9357	0.9341	0.9512	0.9367
Washing down	0.9279	0.9239	0.9425	0.9455
Reaming	0.9356	0.9259	0.9417	0.9329
Washing up	0.9416	0.9518	0.9625	0.9658
Back reaming	0.9518	0.9638	0.9431	0.9839
Tripping out	0.9029	0.8859	0.9035	0.9158
Tripping in	0.9153	0.8967	0.9015	0.9217

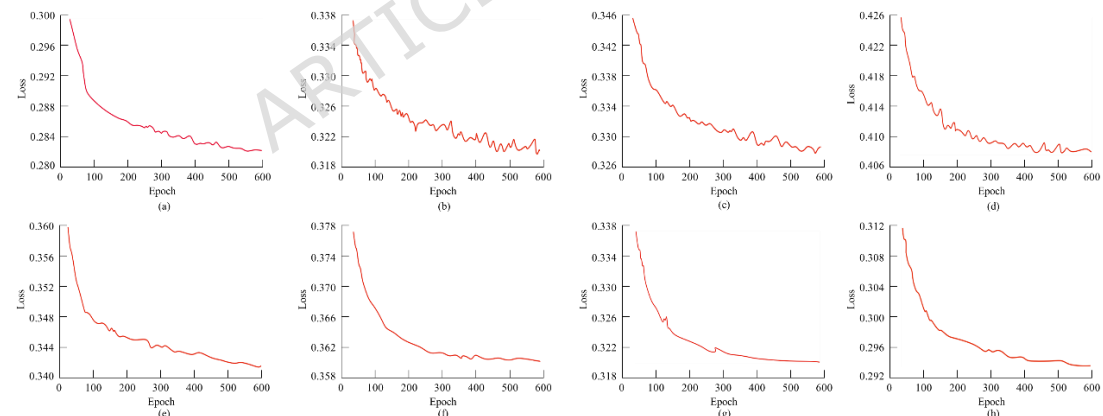


Fig. 7 Changes in loss during the training process under various conditions. (a) Rotary drilling; (b) Slide drilling; (c) Washing down; (d) Reaming; (e) Washing up; (f) Back reaming; (g) Tripping out; (h) Tripping in

5.2 The experimental results of LSTM

The experimental results of the LSTM neural network model are presented in Table 8. As shown in the results, the average F1-Score reached 0.9741, and the accuracy for all drilling conditions exceeded 95%. This demonstrates that the LSTM neural network, which leverages time-series features, can better distinguish corresponding drilling conditions by extracting temporal information from drilling data.

Table 8 Evaluation results of LSTM model

Drilling conditions	Accuracy	Precision	Recall	F1 score
Rotary drilling	0.9721	0.9684	0.9760	0.9721
Slide drilling	0.9743	0.9631	0.9865	0.9746
Washing down	0.9566	0.9255	0.9930	0.9580
Reaming	0.9848	0.9715	0.9989	0.9850
Washing up	0.9803	0.9657	0.9960	0.9806
Back reaming	0.9910	0.9871	0.9950	0.9910
Tripping out	0.9223	0.8962	0.9551	0.9247
Tripping in	0.9259	0.9055	0.9228	0.9355

5.3 Comparison of algorithm results

The primary goals of optimizing drilling operations are to minimize time consumption during condition identification and to maximize the accuracy of predictive methods, two standard metrics for evaluating performance, as compared in Table 9. A significant challenge arises because non-essential activities can account for 30% of total operational time. Consequently, the accurate real-time identification of drilling conditions and the reduction of such non-productive time are fundamental to lowering costs and improving overall efficiency. However, conventional approaches that depend on expert interpretation or theoretical deductions are often hampered by subjective bias, a reliance on scarce expertise, and inherent time delays.

A comparative analysis of the CNN, BP, and LSTM models on the drilling dataset is presented in Table 9 and Fig. 8. In terms of classification accuracy, LSTM achieved the highest mean F1-Score of 0.9741, outperforming BP (0.9694) and CNN (0.962). This performance advantage is corroborated by its computational efficiency. The LSTM model completes condition identification in 6.9 seconds on average, which is notably faster than BP (10.6 s) and CNN (13.8 s), indicating a substantial margin of efficiency.

Table 9 Comparison of algorithms and models

Indicator	Model	Rotary drilling	Slide drilling	Washing down	Reaming	Washing up	Back reaming	Tripping out	Tripping in
Accuracy	CNN	0.8556	0.9023	0.9156	0.9016	0.8859	0.8936	0.8652	0.8529
	BP	0.9261	0.9357	0.9279	0.9356	0.9416	0.9518	0.9029	0.9153
	LSTM	0.9721	0.9743	0.9566	0.9848	0.9803	0.9910	0.9223	0.9259
Precision	CNN	0.8723	0.8958	0.9034	0.9126	0.9011	0.8861	0.8925	0.8639
	BP	0.9236	0.9341	0.9239	0.9259	0.9518	0.9638	0.8859	0.8967
	LSTM	0.9684	0.9631	0.9255	0.9715	0.9657	0.9871	0.8962	0.9055
Recall	CNN	0.8962	0.9124	0.9065	0.9139	0.8992	0.9214	0.8859	0.9163
	BP	0.9433	0.9512	0.9425	0.9417	0.9625	0.9431	0.9035	0.9015
	LSTM	0.9760	0.9865	0.9930	0.9989	0.9960	0.9950	0.9551	0.9228
F1 score	CNN	0.8981	0.9251	0.9168	0.8995	0.9284	0.9197	0.8998	0.9201
	BP	0.9518	0.9367	0.9455	0.9329	0.9658	0.9839	0.9158	0.9217
	LSTM	0.9721	0.9746	0.9580	0.9850	0.9806	0.9910	0.9247	0.9355

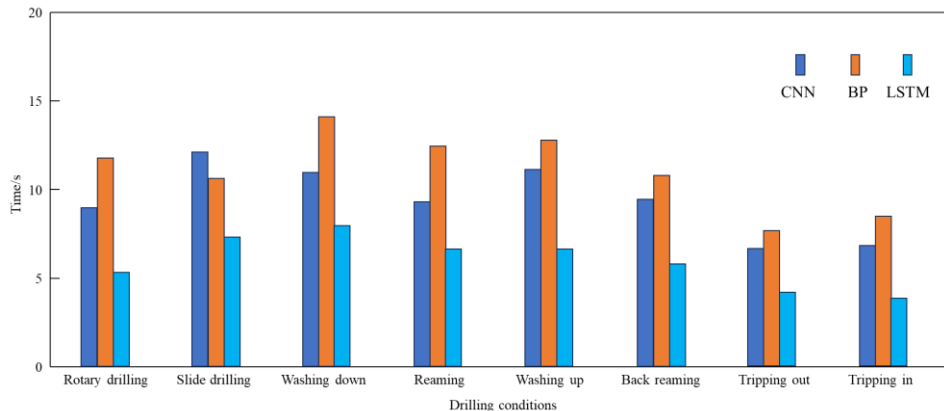


Fig.8 The comparison of consuming time between different models

5.4 Feasibility and Future work

The traditional method for identifying working conditions is limited by issues such as data collection and geological conditions. It fails to deeply explore the intrinsic connections of drilling data changes, making the traditional method difficult to be widely applied. By comparing the recognition effects of BP, CNN, LSTM model, it was found that LSTM was capable of extracting information from long-term sequences and had better recognition effects than CNN, but performed poorly in recognizing dense and repetitive conditions. Owing that the identification system was being studied, the predicted cases were conducted based on the established models. Presently, it was being studied more focused on the method and test. It still needed time to develop the comprehensive identification system integrating these models and then was applied in the drilling. The MS proposed the new idea on the identification of drilling conditions and this idea has been validated. Subsequently, it could help accelerate the research of the identification software based on the LSTM model and be popularized on the real-world drilling operations.

While intelligent drilling methods show promise, they still require further refinement. Surface sensors at drilling sites are subjected to prolonged exposure to wind, sunlight, rain, and moisture, causing internal electronic components to degrade prematurely. As a result, the quality of drilling parameter curves may decline continuously or intermittently. Artificial intelligence algorithms, unable to distinguish between authentic data artifacts and true anomalies, often generate false alarms. To address these issues, the following recommendations are proposed:

1) Enhance the monitoring system. In areas where logging curves cannot reliably identify operational conditions, it is advisable to integrate image or video recognition technology. This would enable comprehensive oversight of onsite activities and facilitate the development of distinct early-warning models for various drilling scenarios. Such an approach would help eliminate ambiguities where a single data source corresponds to multiple potential interpretations.

2) Improve sensor performance. Upgrading sensor sealing and adopting components with

proven stability in harsh environments is essential. These measures will help ensure the authenticity and reliability of source data.

3) Strengthen system training and algorithm development. Although artificial intelligence has been introduced into drilling engineering in recent years, and numerous researchers and experts have explored its use for early warning and incident management, most applications remain in preliminary stages. Given the complexity of drilling processes and the demanding hardware environment, continued efforts should focus on refining algorithms to filter interference and on developing adaptable solutions for diverse operational and environmental conditions.

6 Conclusions

(1) Four evaluation metrics, such as accuracy, precision, recall, and F1-score, were adopted to assess the classification performance of the machine learning models. The generalization error was selected to evaluate the model performance, where a smaller generalization error indicates better model performance.

(2) To ensure that the selected drilling condition parameters are independent yet exhibit a certain degree of correlation, Pearson correlation coefficient analysis was conducted. This analysis identified eight drilling parameters from the comprehensive logging data as input variables for network training: well depth, bit position, hook height, hook load, weight on bit, rotational speed, torque, flow rate, and standpipe pressure.

(3) A comparative analysis of the strengths and weaknesses of three algorithms, traditional CNN, BP, and LSTM, revealed that the LSTM outperforms both the CNN and BP in drilling condition classification. This demonstrates the unique advantage of LSTM in handling long-time-series, high-dimensional, nonlinear complex mapping relationships.

Acknowledgements We acknowledge the contribution of all authors on the whole MS.

Funding Funding was supported by Research on Automated Crawler Core Drilling Equipment and Process Technology (E210100721).

Data availability The datasets generated and analysed during the present study are not publicly available because of applicable institutional guidelines but are available from the corresponding author upon reasonable request.

Declarations

Ethics approval and consent to participate

Not applicable.

Consent for publication

Not applicable.

Competing interests

All authors declare no conflict of interest.

References

1. Li YF, Zhang B, Sun WF. Research on intelligent early kick identification method based on SVM and D-S evidence theory. *Drilling & Production Technology*. 2020; 43(5): 27-30.
2. Yang J, Sun T, Zhao Y. Advanced real-time gas kick detection using machine learning technology. *SPE, The 29th International Ocean and Polar Engineering Conference*. 2019.
3. Ahmed A, Kenneth OA. Experimental analysis of drillstring vibrations using a small-scale drilling rig. *Nonlinear Dynamics*. 2025; 113, 17491-17518.
4. Javokhirbek Z. Tribological failure analysis of tungsten carbide tool inserts used in drilling operations. *Journal of Failure Analysis and Prevention*. 2025; 25, 2282-2289.
5. Mehrbod K, Bagherpour M. An intelligent approach to predict the drilling penetration rate using acoustic emission technique (AET). *Scientific Reports*. 2025; 15, 37457.
6. Adwani A, Mubarak, Nguyen. *Advancements in Salt Inhibitor Flush for Controlling Blockage in Production Lines*. 2025; 5, 200655.
7. Osarogiagbon A, Muojeke S. A new methodology for kick detection during petroleum drilling using long short-term memory recurrent neural network. *Process Safety and Environmental Protection*. 2020; 142: 126-137.
8. Muojeke S, Venkatesan R. Supervised data-driven approach to early kick detection during drilling operation. *Journal of Petroleum Science and Engineering*. 2020; 192: 107342.
9. Sun T, Zhao Y, Yang J. Real-time intelligent identification method under drilling operation conditions based on support vector machine. *Petroleum Drilling Techniques*. 2019; 47(5): 28-33.
10. Hou XX. Identification and time effect analysis of drilling conditions based on logging data. *China University of Petroleum*. 2022.
11. Liu G. *Drilling complex self-adaptive intelligent warning model and its application*. Xi'an Shiyou University. 2018.
12. Liu SW, Cao XH. An intelligent identification method for drilling conditions based on decision tree. *The Journal of New Industrialization*. 2022; 12(1): 28-30.
13. Mao GQ, Song XZ, Ding Y. Drilling condition identification method based on gradient boosting decision tree. *Oil Drilling & Production Technology*. 2023; 45(5):532-539.
14. Rostamian A, Heidaryan E, Ostadhassan M. *Evaluation of different machine learning frameworks to predict CNL-FDC-PEF logs via hyperparameters optimization and feature selection*. *Journal of Petroleum Science and Engineering*. 2022; 208: 109463.
15. Zhang FF, Cui YH, Yu C. Recent development and future trends of drilling status recognition technology based on machine learning. *Journal of Yangtze University (Natural Science Edition)*. 2023; 20(4): 53-65.
16. He M, Chen H, Zhang DS. Research on intelligent identification of drilling conditions based on deep auto-encoder. *Journal of Yangtze University (Natural Science Edition)*. 2023; 20(3): 84-93.

17. Wei G, Xiao L, Li S. Identification methods for drilling conditions based on transformer neural network. *Petroleum Drilling Techniques*. 2025; 54(3): 33-41.